January 2018

Proteolipid Protein 1 Regulates Inflammation In The Central Nervous System

Whitney Hoff
Wayne State University, whitney_lee16@yahoo.com

PROTEOLIPID PROTEIN 1 REGULATES INFLAMMATION IN THE CENTRAL NERVOUS SYSTEM

by

WHITNEY HOFF

THESIS

Submitted to the Graduate School

of Wayne State University,

Detroit, Michigan

In partial fulfillment of the requirements

for the degree of

MASTER OF SCIENCE

2018

MAJOR: MOLECULAR GENETICS AND GENOMICS

Approved by:

_____

Advisor Date

DEDICATION

I dedicate this thesis to the state of Michigan and the 5 and ½ years I have spent here. I will be forever grateful for this time and all I have gained.

ACKNOWLEDGEMENTS

Thank you, thank you to Dr. Robert Skoff for putting up with me for these years and for allowing me to be a part of his lab. He has truly helped me to grow as a scientist through his mentorship. He has been very patient with me as I've learned that "microglial" is an adjective and not a noun and that *Plp1* must ALWAYS be in italics. Mostly I'm grateful for the warm environment his lab has provided me with as I have spent time learning and growing.

Many many many MANY thanks to my friend and colleague Denise Bessert-Collins for being the nicest, most warm-hearted person I have ever met. She has taught me everything I know about every lab technique and every experiment I've needed to complete this work. She has been a constant support. Thank you also to Malika Somayajulu-Nitu, Fayi, Yao, Joshua Brady, and Parth Hindu for making work more fun by being a part of the lab for at least part of the time I was there.

I would also like to acknowledge my committee members: Drs. Alex Gow, Joyce Benjamins, Gregory Kapatos, and Maik Hüttemann. Thank you for all the hours you have given up meeting with me and for all the advice you offered.

Last of all, thank you to my family and to my friends who have become family as I've been far away from my own. Thank you for helping me to practice for each presentation I've had to give, thank you for reading over the grant applications and the manuscripts I have written. Thank you for your genuine interest in my work and your encouragement to continue forward. Thank you to my Anthony and my Lucy for being there at the end and reminding me what is most important.

TABLE OF CONTENTS

LIST OF FIGURES

CHAPTER 1: INTRODUCTION

Myelin and the Central Nervous System

In 1543 Andreas Vesalius mapped the brain and therein described what he termed then “white matter” and “grey matter” areas. Thus, began the study of myelin sheaths in the central nervous system (Boullerne et al, 2016). In the nearly 500 years that have followed, much progress has been made. Advancements in technology have allowed scientists to make discoveries regarding myelin that Vesalius would have never thought possible.

Early studies of myelin focused on elucidating the form and function of myelin sheaths. It wasn’t until 1925 that Ralph Stayner Lillie suggested that myelin is necessary for the rapid propagation of action potentials through the nervous system via saltatory conduction and it was well after WWII that myelin’s function as an insulator was confirmed (Boullerne et al, 2016).

The origin of myelin was not confirmed until the mid-1950’s, and the function of oligodendrocytes was not found until 1962. This was 50 years after oligodendrocytes were first described by Pio del Rio Hortega (Boullerne et al, 2016). Prior to this time, it was believed that myelin was formed directly by axons. This discovery changed the face of myelin research in the central nervous system (CNS) henceforth.

Myelination is a multistep process that begins with the generation and proliferation of oligodendrocyte precursor cells (OPCs) (Snaidero and Simons, 2017). OPCs differentiate from cells that originate in the ventricular zones in the brain. The differentiation of OPCs into mature oligodendrocytes is a process that occurs over time and involves genetic, biochemical, structural, and physiological changes within the cell.

The expression of developmental markers allows OPCs to differentiate into phenotypically different types of mature oligodendrocytes that have varying functions throughout the white and grey matter of the CNS. There are 4 types of myelinating oligodendrocytes (Butt et al, 1995) that can be identified through morphological differences.

Oligodendrocyte's primary purpose within the CNS is myelination of axons. Unlike the myelinating cells of the peripheral nervous system (PNS), oligodendrocytes can myelinate multiple axons at a time. Oligodendrocytes ensheath small and large diameter axons in a multi-lamellar fashion, with the leading edge at the inner tongue around the axon and moving outward. This process requires the production of a variety of proteins that are needed at different times throughout the process for a variety of tasks (Snaidero and Simons, 2017). Any disruption of the CNS myelin, either through injury, pathological degeneration, or genetic intervention (Nave et al, 1994) leads to severe functional deficits and disease.

Proteolipid Protein 1 and Pelizaeus-Merzbacher Disease

The *Plp1* gene codes for Proteolipid Protein 1 (PLP) whose structure is preserved across species. The gene is 17.4 kb long and is located on chromosome Xq22.3 (Boison and Stoffel, 1994). PLP (276 amino acids) and its isoform DM20 (which lacks 35 amino acids specific to PLP) are tetraspan membrane proteins whose expression are highly regulated during brain development because they play a major role during the myelination of the CNS (Readhead et al, 1994). PLP/DM20 are the most abundant proteins in CNS, making up approximately 50% of the protein mass in the myelin. PLP is most highly expressed by oligodendrocytes and seems to play a major role in the structural stability

of myelin sheaths formed by these cells (Campagnoni and Skoff, 2001) by functioning in spiral wrapping, membrane compaction, and the fine architecture of multilayered sheath (Klugmann et al, 1997). However, these proteins are expressed elsewhere as well and are known to function in the regulation of apoptosis throughout the body, especially during development (Skoff, 2004). It is suspected that not all roles of PLP are known and understood as this protein is complex pathogenically (Klugmann et al, 1997).

Pelizaeus-Merzbacher disease (PMD) results from proteolipid protein 1 (*PLP1/Plp1*) gene mutations. PMD is a rare, x-linked, hypomyelinating disease characterized by delayed motor and cognitive development, nystagmus, ataxia, hypotonia, and spasticity (Seitelberger et al, 1995; Garbern, 2007). *PLP1/Plp1* mutations fall into four categories: duplications, point mutations, deletions, and frameshift mutations (Hüttemann et al, 2009) each of which affects the severity and onset of PMD. Therefore, PMD has been divided into 2 subtypes (Nave and Boespflug-Tanguy, 1996): 1) The connatal form, resulting primarily from *PLP1* point mutations, is the most severe form of PMD and usually leads to death within the first decade. 2) The classic form, which results from *PLP1* duplications, is the most common form (50-75% of cases) and onsets at around two months of age. Those affected can live several decades with variable neurological deficits (Koeppen et al, 2002).

The mildest form of PMD, often confused with spastic paraplegia type 2 as it is not always possible to discriminate between them, results from *PLP1* null mutations (Garbern, 2007). This form of the disease can manifest during the teenage years, and although the effected males present a much milder phenotype when compared to patients/model animals with *PLP1/Plp1* mutations or missense mutations, patients still

have a shortened lifespan (Raskind et al, 1991; Inoue et al, 2002). *PLP1*/*Plp1* null mutations result in a lack of synthesis of PLP and although PLP constitutes 50% of myelin protein, myelin still forms and is essentially normal (Klugmann et al, 1997). This results in a clinically distinct disorder from the classic forms of PMD that is often ignored because of it mild phenotype.

Because of differences resulting from the variety of *PLP1/Plp1* mutations, care should be taken not to generalize observations found in *PLP1/Plp1* null cases with other PMD subsets as pathogenic findings are unique to each mutation. Therefore, describing the central pathologic differences between *PLP1* mutation types in humans is worthy of attention because it could lead to a more refined discussion on future therapies (Laukka et al, 2016).

PLP and Inflammation: M1 vs M2

In many neurodegenerative diseases, microglial activation and an inflammatory response have been described (i.e. Parkinson's and Alzheimer's). It is known that changes in expression of myelin proteins, specifically PLP, are associated with progressive massive microglial inflammation in animal models of PMD (Bachstetter et al, 2013; Tatar et al, 2010; Ip et al, 2006). Activation of the innate immune system, particularly of astrocytes and microglia, is mostly associated with the deleterious role of neuroinflammation and could contribute to neuronal death in PMD patients. Studies in *Plp1*tg and *jimpy* mice have enabled the unmasking of a strong inflammatory environment when PLP is duplicated (*Plp1*tg) or mutated (*jimpy*) characterized by extensive microglial activation, up-regulation of pro-inflammatory cytokines (Tatar et al, 2010) and involvement of T-cells in myelin degeneration (Ip et al, 2006). Years of study has brought

to realization that neuroinflammation is not restricted to PMD animal models, but that it is also *likely* a significant hallmark of PMD in humans (Skoff, unpublished data). Drs. Carrie Tatar and Robert Skoff to studied inflammation specifically in the *Plp1*tg mice. They found intense microglia reactivity and an up-regulation of many pro-inflammatory cytokines and chemokines (Tatar et al, 2010). Causal links have been determined have been suggested between insertion of PLP into mitochondria, metabolic abnormalities, changes in the extracellular fluid, microglia activation, and neurodegeneration in *Plp1*tg mice (Appikalta et al, 2013). The increased production of proinflammatory cytokines by microglia in these mice, along with their typical amoeboid morphology implies a M1 (or classical) inflammatory response in these animals.

M1 microglia are characterized by their amoeboid shape, high motility, strong phagocytic capacity, and production and release of pro-inflammatory cytokines and chemokines (Du et al, 2017). These cells are otherwise known as “classical” microglia and have long been thought to be the primary type of activated microglia cell. These cells are known for their ability to kill/fight (Rath et al, 2014). They are associated with TLRs, NODs, and NOD like receptors that respond to TNF-α, IL-6, IL-1b, and INF-γ. They produce ROS and NOS (specifically iNOS), both of which attribute to the death of surrounding cells (Cherry et al, 2014). Because of this, iNOS is often used as a marker specific to M1 microglia cells.

Microglial activation has classically been considered destructive, however, in many disease states these cells are known defenders. Since the immune system functions to protect the brain it is logical to propose that the primary function of microglia is protective (Chen and Trapp, 2016). This leads us to the other end of the of the microglial spectrum:

M2 microglia cells. These cells are known for their healing/fixing properties (Rath et al, 2014). They can suppress neuroinflammation, restore homeostasis and help protect the brain (Chen and Trapp, 2016). The classification of these cells is more complex as they are any cells that show a response ”alternative” to the classic M1 response. This variation in response is based of varying environmental clues. Often the production of anti-inflammatory cytokines/chemokines such as IL-4, IL-13, and IL-10 is associated with an M2 response (Cherry et al, 2015). M2 cells are generally characterized by thin cell bodies and branched processes (often referred to as transitional morphology) (Du et al, 2017). Arg1 is commonly used as a marker for these cells. Both Arg1 and iNOS originate from arginine, thus Arg1 is a iNOS competitor that pushes microglia towards the M2 phenotype (Cherry et al, 2014).

Unlike that found in the *Plp1*tg mice, *Plp1*ko mice seems to adopt a more beneficial, anti-inflammatory (likely M2) phenotype, that could explain the benefits of *Plp1* deletion vs *Plp1* duplication.

Hypothesis and Aim of Research

Aim of Research: Investigate how abnormal expression of PLP in oligodendrocytes directly or indirectly leads to activation of an inflammatory response and, in turn, cell death in mouse models. This study focused on measurement of the inflammatory response in *Plp1*tg, wt*Plp1*, and *Plp1*ko mice. I quantified overall microglial cell number, cell morphology, and branching. Cells were further characterized through measurement of cytokines and chemokines at mRNA and protein levels to determine whether they had a destructive (M1) or protective (M2) function in the CNS of *Plp1*ko mice.

Previous studies have shown that PLP is inserted into the mitochondria of oligodendrocytes of *Plp1*tg and wt*Plp1* mice (Hüttemann et al, 2004). The mechanisms through which PLP is inserted into oligodendrocyte mitochondria via the Mia40/Tom40-Erv1 pathway is understood. Based upon PLP's co-localization with creatine kinase (Hüttemann et al, 2004), it appears to be present in the inter-membrane space. PLP has motifs (C_X3C and C_X9C) in its N-terminus (C6, C10, C25, and C35) that match the Mia40/Tom40-Erv1 relay system used to transport proteins into mitochondria. Mutation of any of these cysteines blocks PLP from being inserted into the mitochondria of oligodendrocytes (Hüttemann et al, 2004). When the *Plp1* gene is duplicated, this insertion results in metabolic defects: a decrease in mitochondria membrane potential (Hüttemann et al, 2004) and acidification of media and extra cellular fluid through and increase in ATP (Appikalta et al, 2014). These phenomena are quite different from the commonly accepted view that PLP is exclusively a myelin adhesive protein and that the pathology in the PLP mutants is due to demyelination and/or hypomyelination. It is likely that wild type PLP plays an important role in mitochondrial function and that improper titration leads to a diseased state in the form of microglial activation (Tatar et al, 2010). Current data suggest PLP plays a role as a protein channel in mitochondria (Skoff, unpublished data).

This activation, in turn, likely contributes to the extensive neuronal degeneration described in humans and mice that have *PLP1/Plp1* gene duplications. *Plp1*ko mice experience less oligodendrocyte apoptosis than either wt*Plp1* or *Plp1*tg mice (Skoff et al, 2004). I **hypothesize** that activated microglia in these *Plp1*ko mice may play an alternative, protective, role.

CHAPTER 2: THE INFLAMMATORY RESPONSE IN *Plp1*KO MICE VS *Plp1*TG MICE

EXPERIMENTAL DESIGN AND METHODS

Animals

Two transgenic mouse colonies, kindly provided by Dr. Klaus Nave, were used for this study. One with a duplication the *Plp1* gene exhibiting at least a twofold transcriptional over-expression of *Plp1* (*Plp1*tg line #66) (Readhead et al, 1994) and another in which the *Plp1* gene is not expressed (*Plp1*ko) (Klugmann et al, 1997). Two control mouse colonies, B6129 for *Plp1*ko and C57BL/6 for *Plp1*tg (Jackson Laboratory, Bar Harbor, ME, U.S.A.), were used as well. Male and female *Plp1ko* mice and B6129 controls were used at 1, 3, and 6 months of age. *Plp1*tg mice and C57BL/6 controls were used at 1 month of age as the lifespan of the *Plp1*tg mice is less than three months.

All mice were obtained from our breeding colonies (where the lines have been maintained for 15 years) housed in the Division of Laboratory Animal Resources (DLAR) at Wayne State School of Medicine (Detroit, MI), a federally approved animal facility. All mice were housed in DLAR animal facilities that are under the direct supervision of the Institutional Animal Care and Use Committee (IACUC), a federally approved institutional committee; all procedures were approved by the Wayne State University IACUC.

Genotyping

The genotypes of *Plp1*tg and *Plp1*ko mice were identified by extraction of DNA from tail clips with the Extract-n-Amp kit (Sigma-Aldrich, St. Louis, MO, U.S.A.) between 14 and 21 days. DNA from mice was used to measure expression of the *Plp1* gene. Quantitative PCR was performed with an Eppendorf PCR system using PCR mix from kit and two sets of primers: PLP3F: 5’-ACGAGCAGTGAGAGTTGGGT-3’ and PLP4R:5’-

AGTCTGTTTTGCGGCTGACT-3' and NEO4:5'-GGCTATTCGGCTATGACTGGGC-3' and NEO5:5'-GGGTAGCCAACGCTATGTCCTGA-3' to amplify PLP and the neo cassette. Only the neo band is amplified in homozygous *Plp1*ko mice in males and females. PCR products were resolved on a 1.5% agarose gel and visualized with ethidium bromide.

Iba1 Immunocytochemistry

All rodents used for immunocytochemistry (ICC) were anesthetized with an intraperitoneal lethal dose of chloral hydrate (650 mg/kg body weight) in accordance with Wayne State University IACUC protocols and perfused intracardially with 4% (w/v) paraformaldehyde (PFA) in phosphate-buffered saline (PBS). Whole brains were removed, placed in PFA, and stored at 4°C until further use. Fifty µm transverse sections were cut coronally with a Vibratome, placed in PBS as free-floating sections, and processed for Iba1. Sections were rinsed and mounted on glass slides. Controls for all ICC consisted of sections where the primary antibody was eliminated.

Fifty µm sections from 1, 3, and 6 months old B6129 and *Plp1*ko male and female mice and 1 month C57BL/6 and *Plp1*tg mice were washed with PBS, treated with 3% H_2O_2 for 30 min, washed with PBS, incubated in sodium citrate buffer (10 mM sodium citrate, 0.1% tween) pH 6 for 30 min at 80° C and 30 minutes at room temperature, washed with PBS, treated with 10% Triton-X for 30 min, washed with PBS, blocked with 10% (v/v) goat serum for 30 minutes, washed with PBS, and incubated in polyclonal anti-Iba1 (ionized calcium-binding adaptor molecule 1) antibody (Wako, Richmond, VA, U.S.A.) diluted 1:500 overnight in 0.1 M PBS at room temperature (20° C). Sections were rinsed in PBS and incubated in goat anti-rabbit IgG horseradish peroxidase (HRP;

Jackson ImmunoResearch, West Grove, PA, U.S.A.) conjugated antibody diluted 1:100 and detected using 0.5 mg/ml DAB (diaminobenzidine) (Sigma–Aldrich, St. Louis, MO, U.S.A.). Immunofluorescence was also done using the same protocol exchanging the HRP secondary antibody for goat anti-rabbit ALEXA 594 (Jackson ImmunoResearch, West Grove, PA, U.S.A.)

Three to 6 animals were used for each time point, sex, and strain. For each animal, 3 to 4 matched transverse sections were blindly counted for Iba1 labeled cells using a Leitz (Wetzlar, Germany) Laborlux microscope equipped with a ×50 oil objective and a ×10 eyepiece containing a 1-cm^2 grid divided into 1 mm squares. Cells were counted in the corpus callosum just lateral the ventricle and adjacent to the dorsal inter-hemispheric fissure (Figure 1). The number of cells for each area was summed; averages were determined for each animal and then for each strain. Values represent mean ± SEM of 3 to 4 sections per animals. Data significance was determined using an ANOVA assuming equal variance. This analysis has been completed previously in *Plp1*tg mice (Tatar et al, 2010).

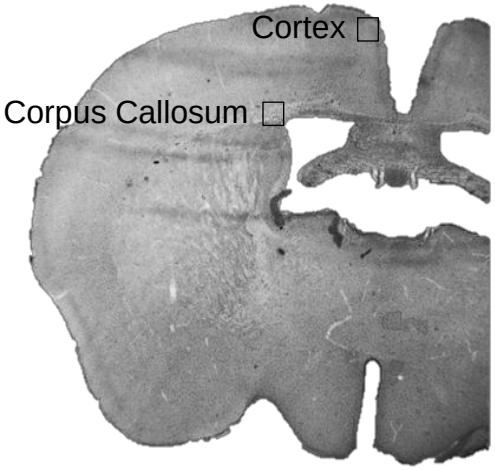

Figure 1: Quantification of Iba1 ICC. Iba1 quantification was completed in 2 areas of the brain. A white matter area in the corpus callosum just lateral the ventricle, and a grey matter area in the cortex adjacent to the dorsal inter-hemispheric fissure on one side. All cells within a 10x10 mm grid were counted.

BrdU/Iba1 Immunocytochemistry

For combined Iba1 and BrdU (bromodeoxyuridine) ICC of wt*Plp1* and *Plp1*ko mice, mice were injected with 100 µg of BrdU/g of body weight intraperitoneally and perfused with 4% paraformaldehyde 70 hours later. This length of interval from injection to sacrifice permits microglia/microglial precursors to divide and differentiate. Brains were removed and 50 µm sections cut coronally using a Vibrotome. Sections were washed in PBS, treated with 2 M HCl for 30 minutes at 37° C, incubated in 0.1 M sodium borate 2x for 30 minutes at room temperature, treated with 3% H_2O_2, incubated in PBS-blocking buffer (PBS containing 0.2% BSA, 0.2% milk and 1.0% Triton) for 30 minutes and incubated with anti-BrdU (BD Biosciences, San Jose, CA, U.S.A.) diluted 1:100 at 4° C overnight. Sections were rinsed in PBS, incubated in an anti-mouse HRP (Jackson ImmunoResearch) conjugated antibody and developed with DAB+cobalt. Sections were then rinsed in PBS and processed for Iba1 immunocytochemistry using DAB (without cobalt) as previously described. This work has been completed previously in *Plp1*tg mice (Tatar et al, 2010).

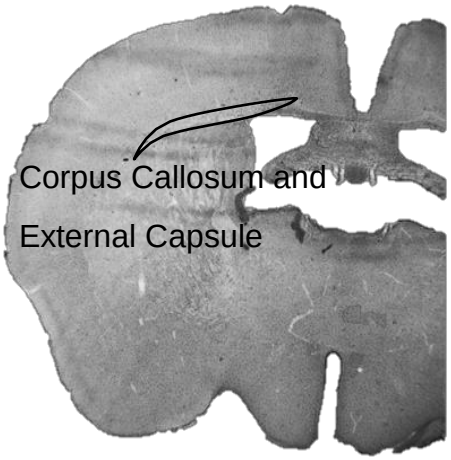

Figure 2: Quantification of BrdU expressing microglial cells. Microglial cells double labeled with Iba1 and BrdU were counted through an oil immersion lens throughout the entire half of the corpus callosum and external capsule.

Quantification was completed as described for Iba1 with only a slight variation. Cells were counted in one entire side of corpus callosum and external capsule (as in

Cerghet et al, 2006; Figure 2). The number of cells for each area was summed and averages determined for each animal and then for each strain. Values represent mean ± SEM of 3 to 4 sections per animal. Data significance was determined using an ANOVA assuming equal variance.

Quantification of Microglial Activation

Using sections treated with Iba1 (as above), microglial activation was quantified based on number of microglial processes and the complexity of branching (Karperien et al, 2013.) Cells with more than 4 processes were counted as ramified (inactive) cells, those with 2-4 processes were counted as transitional cells, and those with less than 2 processes were counted as amoeboid (Figure 3). "Transitional" describes any cell that is between the ramified stage and the amoeboid stage. At each time point (1, 3, and 6 months), sex, and strain (wt*Plp1, Plp1*ko and *Plp1*tg), 3 to 6 animals were used. For each animal, 3 to 4 matched transverse sections branching patterns of Iba1 labeled cells adjacent the dorsal inter-hemispheric fissure were analyzed using a Leitz microscope as described above.

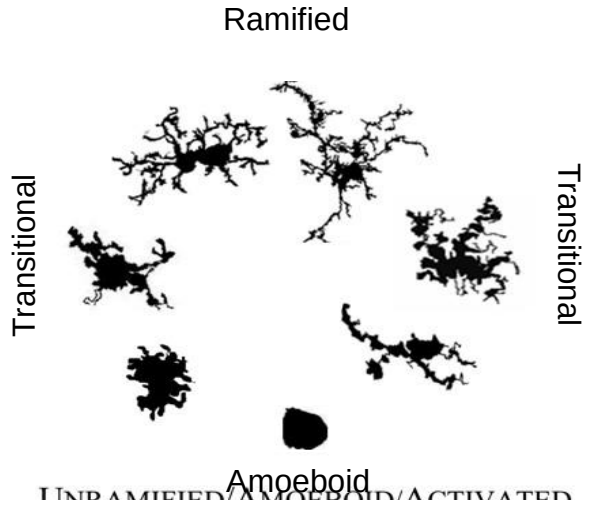

Figure 3: **Various stages of microglial activation based on branching patterns.** Activated cells have fewer branches than inactive cells. *Taken from Karperien 2013.*

Percentage of activated microglial cells in *Plp1*ko and wt*Plp1* male and female mice was verified through double CD68 (activated microglial cell marker) and Iba1 double labelling ICC. 50 µm sections were washed in PBS, treated with 3% H_2O_2, washed with

PBS, incubated in 0.1 M sodium citrate (pH 6) for 15 minutes at 80° C and 15 minutes at room temperature, washed with PBS, and incubated in anti-CD68 (Proteintech, Rosemont, IL, U.S.A.) diluted 1:200 in PBS overnight at room temperature. Sections were washed in PBS, incubated in anti-rabbit HRP (Jackson ImmunoResearch) conjugated antibody and developed with DAB+cobalt. Sections were then treated for Iba1 ICC. Percentage of activated microglia was quantified by counting cells showing CD68/Iba1 colocalization (black and brown staining) as well as all Iba1 labelled cells and determining the percentage of $Iba1^+$ cells also expressing CD68 in the corpus callosum near the ventricle and near the dorsal inter-hemispheric fissure.

Cytokine ELISA

Six 6-month old male *Plp1*ko and wt*Plp1* mice were quickly perfused by transcardial perfusion with cold PBS to remove blood. Brains were removed on ice and placed in sterile tubes. They were then immersed in liquid nitrogen to “snap freeze” and stored at -80° C for later use. One half of each brain was used for the ELISA. Brains were homogenized by addition of 1-3 ml protein extraction buffer (20 Mm Tris-HCL pH 7.5, 150 mM Na_2EDTA, 1 Mm EGTA, 1 % Triton-X, proteinase inhibitor cocktail added freshly, and phosphatase inhibitor cocktail added freshly) and an electric homogenizer. This was done on ice. Brains of both *Plp1*ko and wt*Plp1* mice were homogenized under the same conditions. Homogenates were vortexed and kept on ice for 30 minutes before being centrifuged to remove tissue debris for 20 minutes at 13,000 rpm at 4° C. Supernatants were aliquoted and saved at -80° C. Protein levels were determined by BCA and adjusted to make sure that all samples were the same.

ELISA was run using an inflammatory cytokines multianalyte ELISA from QIAGEN that measures the concentrations of 10 common inflammatory cytokines: IL-1a, IL-1b, IL-2, IL-4, IL-6, IL-10, IL-12, IL-17a, IFN-y, TNF-a, GCSF, and GM-CSF. Samples from 3 *Plp1*ko and 3 wt*Plp1* were run on each plate following the kit protocol. These were compared to samples from *Plp1*tg mice and controls. Data were analyzed, and data significance was determined using an ANOVA by group assuming equal variance.

Arg1/iNOS Western Blot

Three-month-old male *Plp1*ko, *Plp1*tg, and wt*Plp1* (B6129 and C57BL/6) mice were quickly perfused by transcardial perfusion with cold PBS to remove blood. Brains were removed on ice and placed in sterile tubes. They were then immersed in liquid nitrogen to “snap freeze” and stored at -80° C for later use.

Brains were homogenized by addition of 1-3 ml protein extraction buffer (see above) and an electric homogenizer. This was done on ice. All mice were homogenized under the same conditions. Homogenates were vortexed and kept on ice for 30 minutes before being centrifuged to remove tissue debris for 20 minutes at 13,000 rpm at 4° C. Supernatants were aliquoted and saved at -80° C. Protein levels were determined by BCA and adjusted to make sure that all samples were the same.

Western blots were probed with markers for arginase 1 (Protein Tech), iNOS (Protein Tech) and β-actin (Sigma). A standard 4–12% gel was used. Each gel was transferred on to a PVDF membrane, membranes were blocked with 5% (w/v) non-fat powdered milk, incubated in antibody (1:500) overnight in 1% milk, washed with PBS-T, incubated with secondary antibody (1: 10,000) for 1 hour in 1% milk, washed in PBS-T and detected using the ChemiLucent Detection System (Chemicon). Arginase 1 and

iNOS densities were determined using ImageJ software (NIH) and adjusted to β-actin for consistency. Data were analyzed, and significance was determined using a 2-tailed Student's t-test comparisons assuming unequal variance.

Arg1/iNOS Immunocytochemistry

Fifty μm sections from 1, 3, and 6 months old B6129 and *Plp1*ko male and female mice and 1 month C57BL/6 and *Plp1*tg mice were washed with PBS, treated with 3% H_2O_2 for 30 min, washed with PBS, incubated in sodium citrate buffer (10 mM sodium citrate, 0.1% Tween) pH 6 for 20 min at 80° C and 40 minutes at room temperature, washed with PBS, and incubated in polyclonal anti-Arg1 or anti-iNOS antibody (Proteintech, Rosemont, IL, U.S.A.) diluted 1:50 overnight in 0.1 M PBS at room temperature (20° C). Sections were rinsed in PBS and incubated in goat anti-rabbit IgG horseradish peroxidase (HRP; Jackson ImmunoResearch, West Grove, PA, U.S.A.) conjugated antibody diluted 1:100 and detected using 0.5 mg/ml DAB (diaminobenzidine) (Sigma–Aldrich, St. Louis, MO, U.S.A.). Immunofluorescence was also done using the same protocol exchanging the HRP secondary antibody for goat anti-rabbit ALEXA 594 (Jackson ImmunoResearch, West Grove, PA, U.S.A.)

Arg1/iNOS rtPCR and Quantification of mRNA

The transcardial perfusion of *Plp1*ko, B6126, *Plp1*tg, and C57BL/6 mice under anesthesia was performed with pre-cold PBS to remove brain blood. Mouse brain was quickly dissected and kept at -80°C. Half of mouse brain was homogenized in 2 mL of TRIZOL Reagent using a glass-Teflon homogenizer. Following homogenization, insoluble material was removed from the homogenate by centrifugation at 12,000 x g for 10 minutes

at 4° C. Cleared homogenate solution was to a fresh tube. Total RNA purification proceeded following the instruction of TRIZOL® Reagent (Life Technologies).

The iScript™ cDNA Synthesis Kit (Bio-Rad) was used for cDNA synthesis. Each reaction volume included 4 ul of 5x iScript reaction buffer, 1 ul of iScript reverse transcriptase, 1 µg total RNA and nuclease-free water up to 20 ul. Complete reaction mix was incubated 5 minutes at 25°C, 30 minutes at 42°C, 5 minutes at 85°C and held at 4° C. cDNA reaction mix was diluted in 200 ul nuclease-free water.

Eppendorf Realplex 2.0 rtPCR system and Power SYBR® Green PCR Master Mix (Thermofisher) were used to perform real-time PCR. Each real-time PCR reaction included 3 ul cDNA dilution (above), 2 ul primers (iNOS F: GTTCTCAGCCCAACAATACAAGA, iNOS R: GTGGACGGGTCGATGTCAC, Arg1 F: CTCCAAGCCAAAGTCCTTAGAG, Arg1 R: AGGAGCTGCATTAGGGACATC), 5 ul nuclease-free water, and 10 ul Power SYBR Green PCR Master Mix. Reaction mix underwent thermal-cycling as described: 10 minutes at 95°C for Enzyme Activation, denature in 15 seconds at 95°C, and 60 seconds at 60°C for 40 cycles. The $2^{-\Delta\Delta}$CT Method was used for data analysis. Data significance was determined using an ANOVA assuming equal variance.

ATP Measurements in *Plp1ko* and wt*Plp1* Mice

The measurement of ATP in brain was done using a previously published procedure for measuring pH in brain (Skoff et al., 2004). *Plp1*ko and wt*Plp1* mice at 1, 3, and 6 months were sacrificed by cervical dislocation, brains removed and 2-2.5mm sections from the cortex and the corpus callosum were dissected using a razor blade, weighed, and cut into 16 cubes and placed in a vial on ice containing 1ml ice-cold artificial

cerebral spinal fluid (aCSF) (124mM NaCl, 3mM KCl, 3mM CaCl2, 1.5mM MgCl2, 26mM NaHCO3, 1mM NaH2PO4, 10mM D-glucose, and 75μM HEPES) and a magnetic stir bar. Fluid and tissue were gently stirred on a magnetic stir plate for 5 min. Afterwards the contents of the vials were transferred to 1.5ml centrifuge tubes and centrifuged for 1 min. Brain tissue and aCSF was separated and immediately frozen in liquid nitrogen and ATP measured by a member of Maik Hüttemann's lab. ATP of each sample was measured in triplicate, averaged, and then averaged for each group of brains**.** Data was analyzed using an ANOVA by groups to test for significance.

RESULTS

Increased number of microglia in *Plp1*ko mice

Iba1 is a polyclonal antibody that recognizes an ionized calcium-binding adaptor molecule that is only expressed in microglia in the brain (Imai et al, 1996; Graeber et al, 1998; Ito et al, 1998). This antibody has been used to identify microglia in many mammalian species (Tonchev et al, 2003; Yamada et al, 2006). *Plp1*ko mice have significantly more (2-3 fold) $Iba1^+$ microglial cells (indicative of an inflammatory response occurring) in both white and grey matter (Figure 1) of the cerebrum at all time points compared with B6129 control mice ($P<0.05$; Figures 4 and 5). The results indicate that the density of microglial cells is higher in *Plp1*ko mice; increase in density is consistent throughout cerebrum ($P>.05$, Figure 7). It is likely that the increase in microglia in *Plp1*ko mice is even greater than the cell counts indicate because microglia are clustered together making it difficult to determine the exact number of cells.

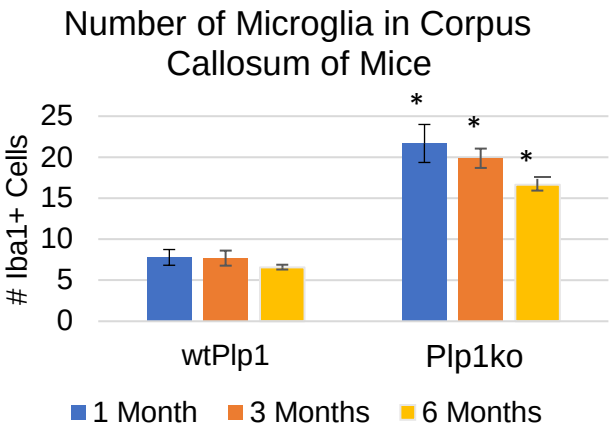

Figure 4: Number of microglia (based on Iba1 ICC) in wt*Plp1* (B6129) and *Plp1*ko at 1, 3, and 6 months of age in the corpus callosum. *Plp1*ko mice have an increased number of microglial cells at all time points when compared to wt*Plp1* mice. Data from males and females combined. N=6. P<.01. ANOVA. * Compares wt*Plp1* to *Plp1*ko at the same time points (colors match).

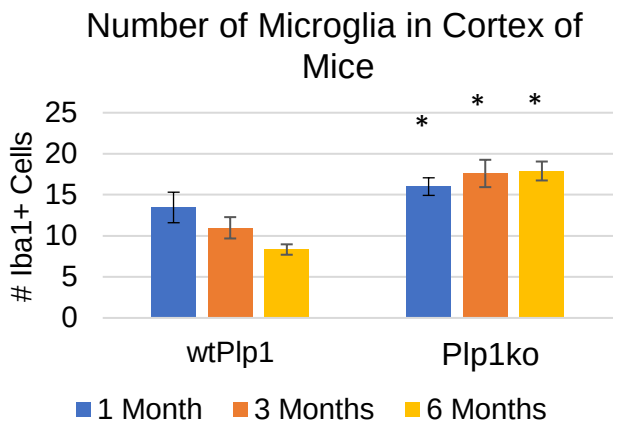

Figure 5: Number of microglia (based on Iba1 ICC) in wt*Plp1* (B6129) and *Plp1*ko at 1, 3, and 6 months of age near the dorsal inter-hemispheric fissure. *Plp1*ko mice have an increased number of microglial cells at all time points when compared to wt*Plp1* mice. Data from males and females combined. N=6. P<.01. ANOVA. * Compares wt*Plp1* to *Plp1*ko at the same time points (colors match).

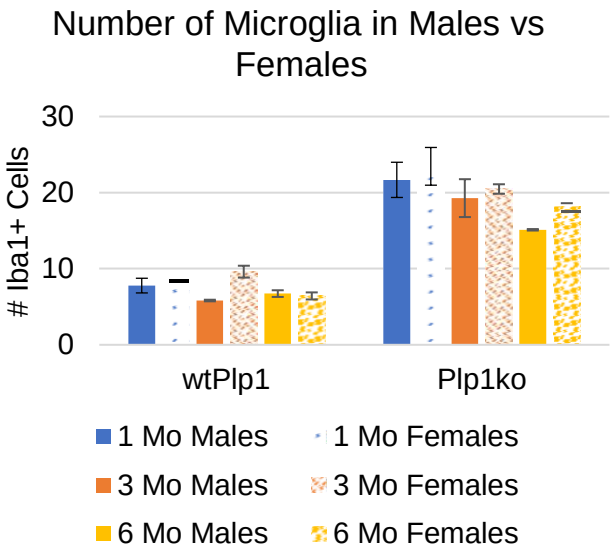

Figure 6: Number of microglia in male and female mice at 3 months compared in corpus callosum. No significant difference in number of microglial cells between males and females in wt*Plp1* (B6129) and *Plp1*ko mice at any time point. N=3. P>.05. ANOVA.

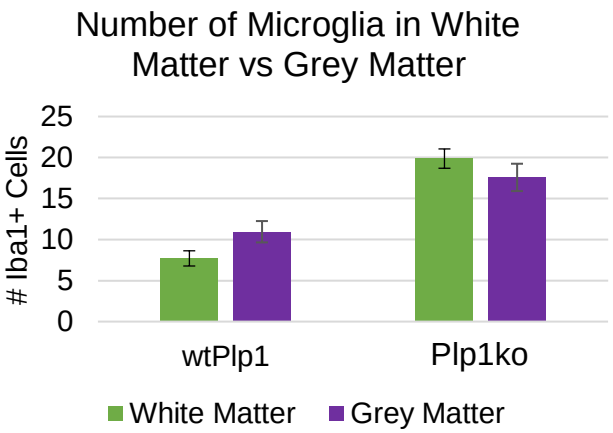

Figure 7: Number of microglia in white matter and grey area compared at 3 months. Comparable areas. No significant difference in number of microglial cells in either wt*Plp1* (B6129) or *Plp1*ko mice at any time point. N=3. P>.05. ANOVA. Same pattern found at 1 and 6 months.

Studies have shown sexual dimorphism exists among glial cells (Cerghet et al, 2009), however in this study, we found no significant difference in number of microglia between males and females in either the wt*Plp1* or the *Plp1*ko mice (P>.05; Figure 6). This insignificance is verified by an ANOVA and is true at all time points: 1, 3, and 6 months.

Increased microglia proliferation in *Plp1*ko mice

Inflammation causes an increase in the proliferation of microglial cells. BrdU is incorporated into cells during the DNA synthesis phase of the cell cycle and can be used to quantify number of proliferating cells throughout the brain. Data from this study shows that in addition to microglial activation being increased in *Plp1*ko, microglia are also stimulated to divide. Combined Iba1 and BrdU ICC was performed on wt*Plp1* and *Plp1*ko cerebra (Figure 8). Figure 8 also shows many $BrdU^+$ cells that are not $Iba1^+$; these cells serve as a control to show that the BrdU-labelled cells are not non-specifically labelled with the Iba1 antibody.

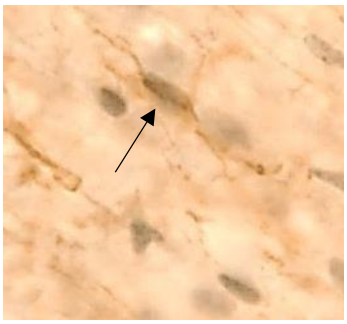

Figure 8: **Iba1/BrdU ICC in a *Plp1*ko mouse.** Iba1 was developed with DAB (brown) while BrdU was developed with DAB+cobalt (black).

All $BrdU^+/Iba1^+$ cells within half of the corpus callosum and external capsule were counted (see Methods and Materials). *Plp1*ko mice have significantly more proliferating microglia cells than wt*Plp1* (3-fold increase) at all time points and in both sexes (Figures

9 and 10). This helps to explain the significant increase in overall microglial cell number in *Plp1*ko mice when compared to wt*Plp1* mice (p<.05, Figure 9).

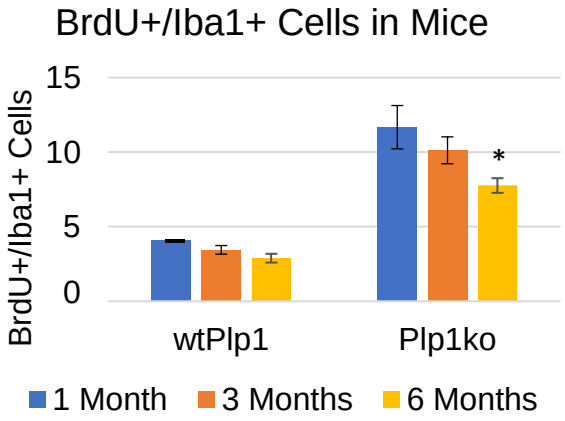

Figure 9: BrdU quantification in wt*Plp1* (B6129) and *Plp1*ko mice at ages 1, 3, and 6 months in corpus callosum. *Plp1*ko mice have an increased number of proliferating microglial cells at all time points when compared to wt*Plp1* mice. Data from males and females combined. N=6. ANOVA. P<.05. * Compares wt*Plp1* to *Plp1*ko (colors match).

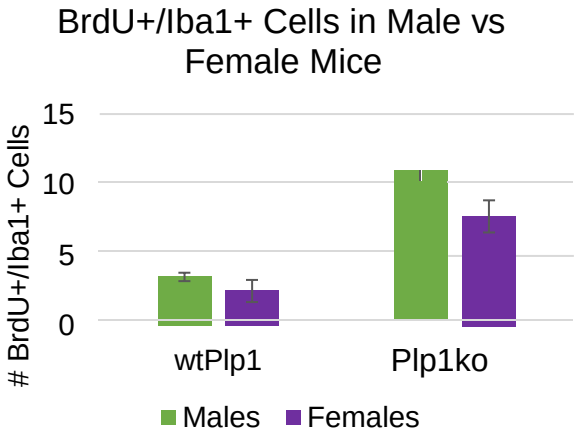

Figure 10: Number of BrdU⁺ microglia in male and female mice at three months in corpus callosum. No significant difference in number of microglial cells in wt*Plp1* (B6129) and *Plp1*ko mice at any time point. N=3. ANOVA. P>.05. Compares like colors. Same pattern found at 1 and 6 months (data not shown).

Microglial activation quantified by number of processes and complexity of branching

Activated microglia change shape as their cell bodies enlarge and become more amoeboid. Cells lose processes and the remaining processes have far fewer branches than those of ramified cells (Figure 3). In this study, activation of Iba1⁺ cells was classified by number of processes and branching complexity (see Methods).

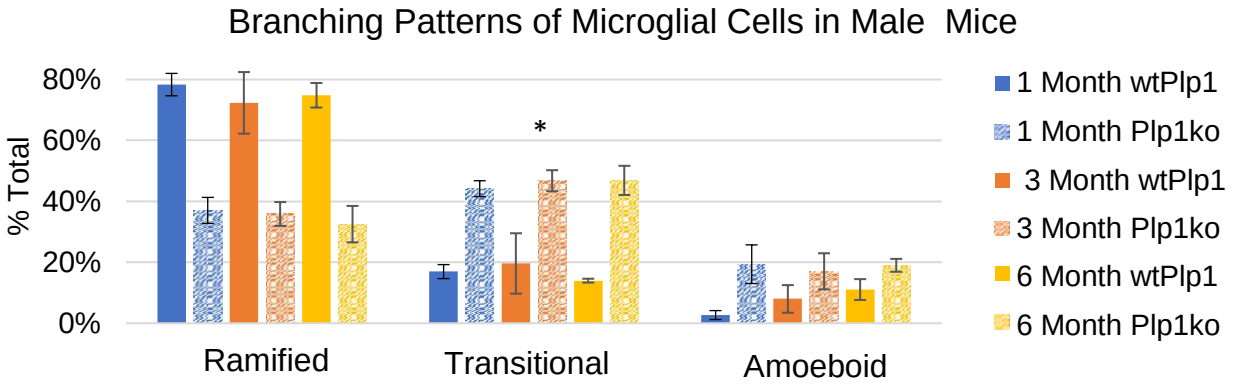

Figure 11: Quantification of microglial activation based on number of processes and complexity of branching patterns at 1, 3, and 6-month old male mice in the cortex near the dorsal inter-hemispheric fissure. Cell activation was quantified based on number of processes branching directly from cell body. 4+ processes=ramified cell, 2-4 processes=transitional cell, and <2 processes=amoeboid. wt*Plp1* mice show mostly ramified cells, while *Plp1*ko mice show mostly primed/reactive cells. Similar data found in females (data not shown) N=3. ANOVA. P<.01 for all groups.

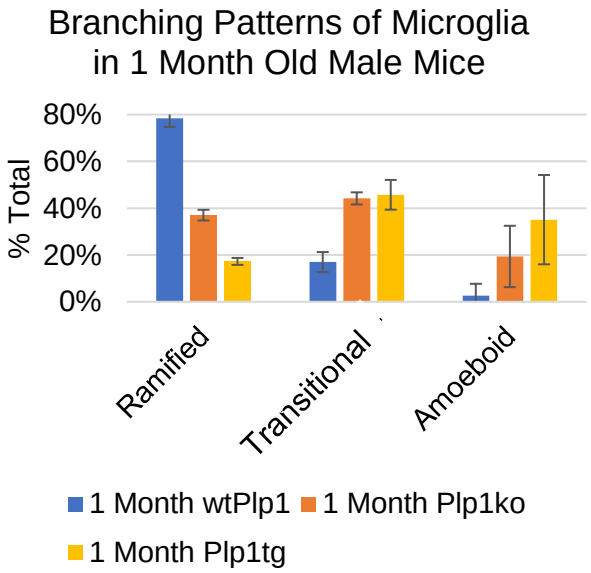

Figure 12: **Quantification of microglial activation in wt*Plp1* (B6129 and C57Bl/6), *Plp1*ko, and *Plp1*tg mice at one month.** *Plp1*tg mice have more amoeboid cells than the *Plp1*ko mice. N=3. ANOVA. *P<.01.

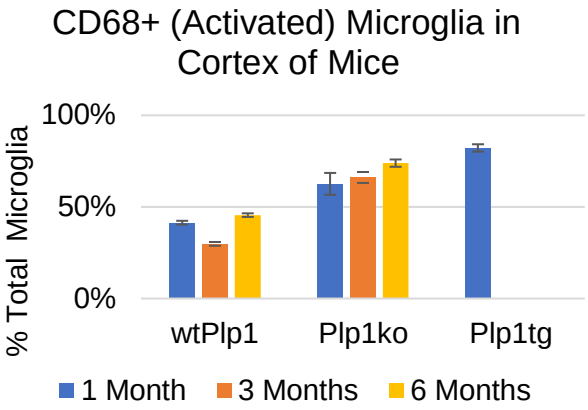

Figure 13: Quantification of CD68^{+} microglial cells near the dorsal inter-hemispheric fissure in wt*Plp1* (B6129 and C57Bl/6) and *Plp1*ko mice at 1, 3, and 6 months and *Plp1*tg at 1 month. Number of activated microglial cells increases from wt*Plp1* to *Plp1*ko to *Plp1*tg. N=6. ANOVA. *P<.01.

Data suggest that wt*Plp1* mice have more ramified microglia than transitional or amoeboid microglia. In contrast, *Plp1*ko mice have a high number of transitional cells compared to ramified or amoeboid microglia (see Figure 11). Both wt*Plp1* and *Plp1*ko mice have relatively few amoeboid cells, especially when compared to *Plp1*tg mice (Figure 12). These differences were found to be significant using an ANOVA and a $p<.01$. These patterns are the same at all time points (1, 3, and 6 months; Figure 11). Analysis was done only in grey matter as in white matter processes extend along the tracts, making it difficult to determine the number of branches.

CD68 ICC was used to verify the percentage of activated microglia cells in *Plp1*ko, *Plp1*tg and wt*Plp1* mice. This protein is localized to the lysosomal membrane in microglia and is up-regulated in actively phagocytic cells. Both M1 polarized and M2 polarized microglia can express CD68 (Walker and Lue, 2005.) Numbers were consistent with those found through branching analysis with wt*Plp1* showing 20-40%, *Plp1*ko showing 60-75%, and *Plp1*tg mice showing around 80% activated microglia cells (Figure 13). Data was found to be significant.

Microglial morphology of *Plp1*ko mice compared to wt*Plp1* and *Plp1*tg mice

Iba1 immunostained microglial cells are present throughout the grey and white matter of both the normal B6129 and the *Plp1*ko mouse. Typical microglia in normal cerebra, often referred to as ramified, have characteristic long and thin processes (Figure 3). Their primary processes are usually twice the length of the axis of the cell body. Secondary processes branch acutely from primary processes, and sometimes tertiary

processes are distinguishable (Tatar et al, 2010). The ramified morphology is similar at all ages in normal B6129 mice (Figure 14)**.**

The morphology and dispersion of microglial cells in the cortical, striatal, and callosal regions of the cerebra in the *Plp1*tg mice differ drastically from that of control mice (Figure 14). Activated microglia in *Plp1*tg are distinguished by coarse short processes and an enlargement of the cell body. Amoeboid microglia have far fewer processes than ramified cells. Microglia are often clustered together and brush-like processes become

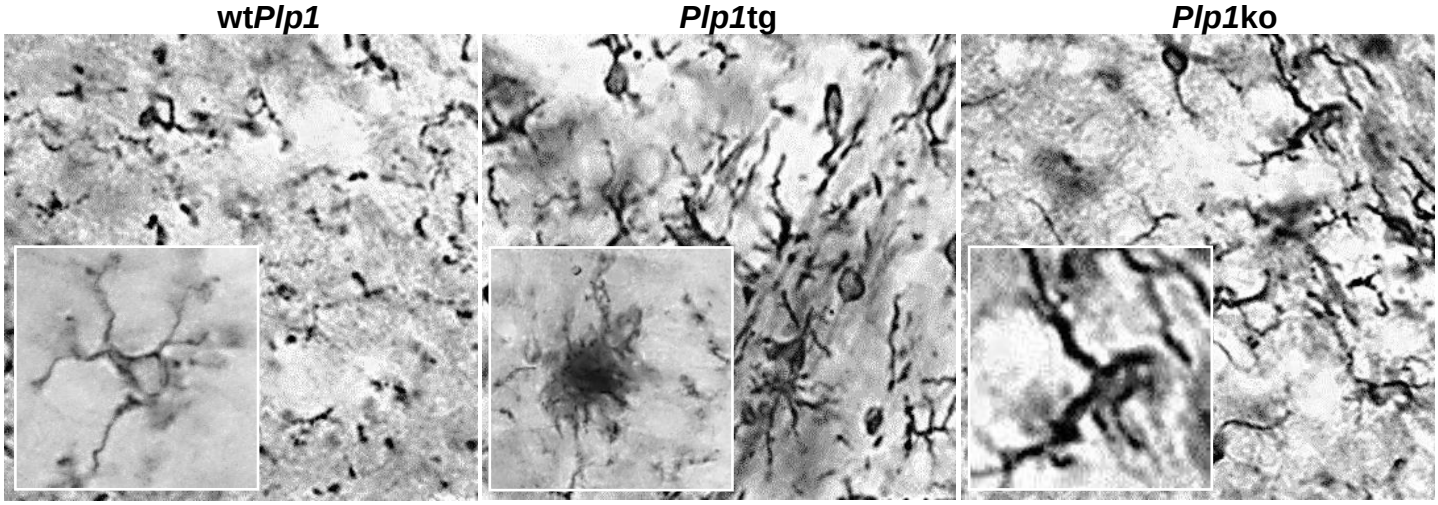

Figure 14: Iba1 ICC of microglia in *Plp1*tg, wt*Plp1*, and *Plp1*ko mice. Cells in *Plp1*tg and *Plp1*ko mice are activated in appearance when compared to wt*Plp1* mice. *Plp1*tg mice act as control examples of activated microglia.

entangled (Tatar et al, 2010).

The morphology and dispersion of microglia cells throughout the brain of the *Plp1*ko mice most closely matches that found in the *Plp1*tg mice (Figure 14). Microglia are clustered together like the cells in the *Plp1*tg mice, but to a lesser degree. Fewer amoeboid microglia are found in *Plp1*ko mice compared to *Plp1*tg mice (Figure 12 and 14). More cells are found to be in the transitional stage with more processes and branches. It is likely that inflammation in *Plp1*ko mice is less severe than in *Plp1*tg mice.

***Plp1*ko Mice Show Decrease in Expression of Pro-Inflammatory Cytokines**

Over activation of M1 microglial cells and excessive amounts of proinflammatory cytokines have been shown to result in neurodegenerative consequences in various diseases such as Alzheimer's, Parkinson's, Huntington's, and multiple sclerosis (Du, 2016). Some examples of proinflammatory cytokines are: IL-1α, IL-1β, IL-6, IL-12, IL-17α, IFN-γ, and TNF-α.

These cytokines are produced or stimulated by M1 (or classical) microglia. Several of these have been shown to be increased in the *Plp1*tg mice (Tatar, 2010). This, along with the massive increase in oligodendrocyte cell death, implies a M1 microglial response in the *Plp1*tg mice. However, the *Plp1*ko mice show either a decrease in the cytokines or no change (see Figure 15) implying an M2 (or alternative) response in these animals. Cytokine levels were measured using a ELISA assay (see methods).

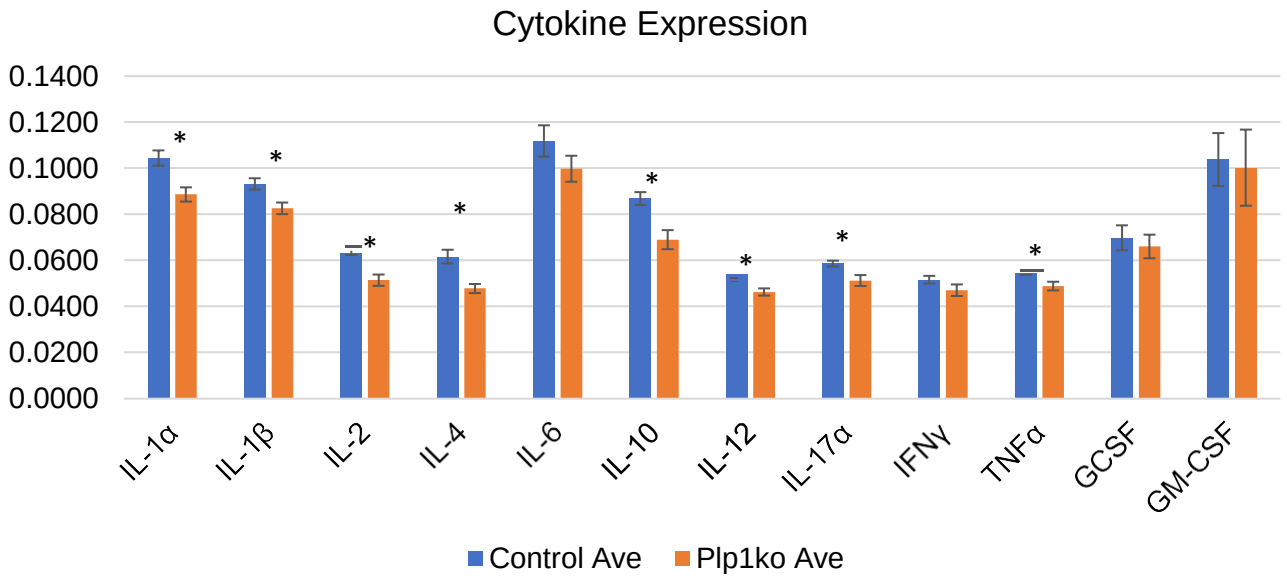

Figure 15: ELISA assay shows decrease in many pro-inflammatory cytokines in *Plp1*ko mice. Compared to wt*Plp1* mice, *Plp1*ko mice show decreased expression of many pro-inflammatory cytokines, such as: IL-1a, IL-1b, IL-12, IL-17a, and TNFa. Decrease in pro-inflammatory cytokine expression implies an alternative phenotype of activated microglia in *Plp1*ko mice. N=5. T-Test, 2 tails. P>.05. Significance indicated by * (orange vs blue).

Microglia in *Plp1*ko Mice Show Alternative (M2) Phenotype Compared to *Plp1*tg Mice

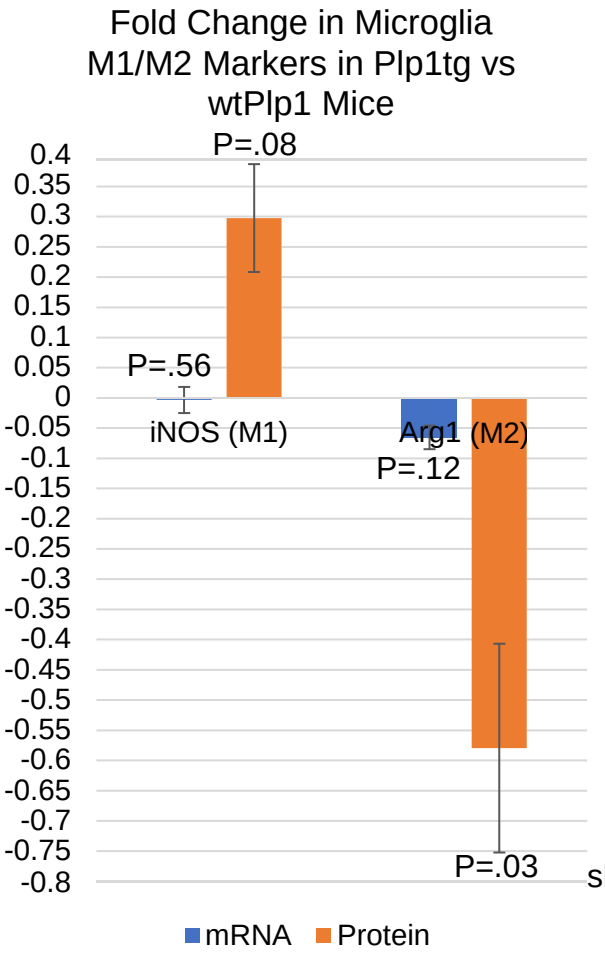

Figure 16. mRNA and protein levels of M1/M2 microglia markers in *Plp1*tg mice. These mice show an increase in iNOS (M1) and a decrease in Arg1 (M2) implying a classical inflammatory response. N=4. P values shown in figure. 2 tailed T-Test.

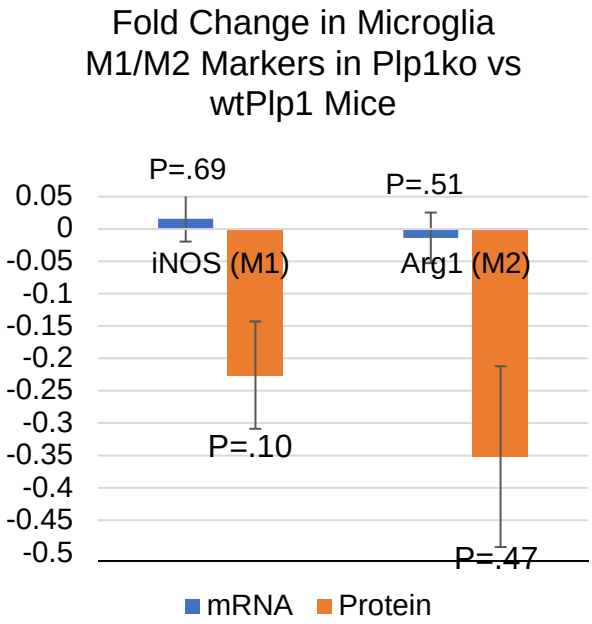

Figure 17. mRNA and protein levels of M1/M2 microglia markers in *Plp1*ko mice. These mice show a decrease in iNOS (M1) and a decrease in Arg1 (M2) implying a something other than a classical inflammatory response. N=4. P values shown in figure. 2 tailed T-Test.

Data led me to believe that *Plp1*ko mice are not experiencing a classical M1 microglia response, but, instead, are experiencing an alternative response. mRNA and Western blot analysis for iNOS (M1 marker) and Arg1 (M2) marker verified this hypothesis. This data is only preliminary and experiments need to be repeated to increase

statistical significance. I need to consider that microglia aren't the only cells that produce cytokines. Astrocytes do as well.

As expected of a classical M1 inflammatory response, microglia in *Plp1*tg mice show an increase in protein levels of iNOS and decreased levels of Arg1 (Figure 16). *Plp1*ko mice show something different (see Figure 17), implying an M2, or alternative response. This helps to explain the benefits of a lack of PLP when compared to mice and humans that overexpress PLP.

ATP Measurements in *Plp1*ko's Do Not Indicate Mitochondrial Dysfunction

Inflammation in *Plp1*tg mice has been linked to mitochondrial dysfunction in the form of increased extracellular ATP (Tatar, et al, 2010). Measurements of extracellular ATP in *Plp1*ko mice do not show the same results (Figure 18). There is no difference found in levels of extracellular ATP found between *Plp1*ko and wt*Plp1* mice. This is likely because PLP plays a role as a protein channel in oligodendrocyte mitochondria and increasing the amount of PLP increases the number of channels, decreasing he amount of ATP leaving mitochondria.

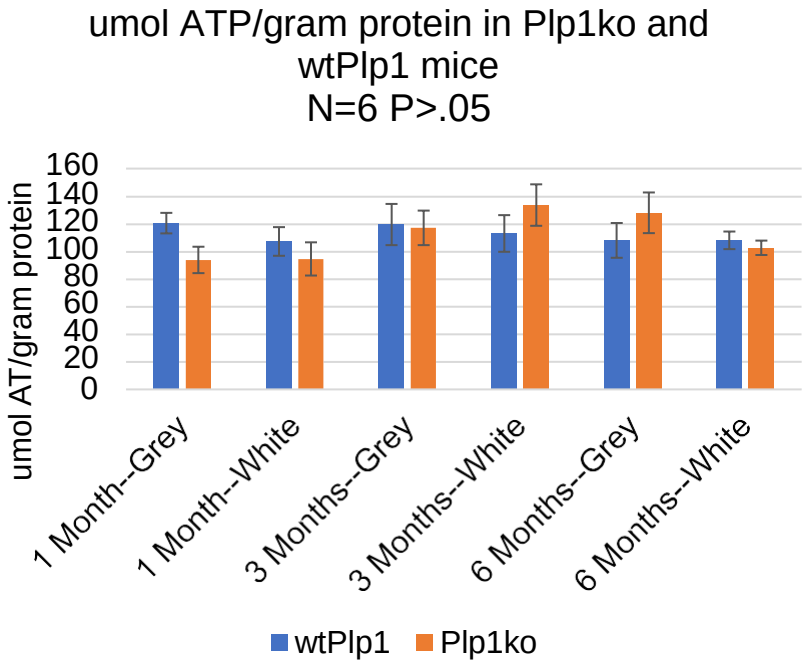

Figure 18. Extracellular ATP levels NOT increased in *Plp1*ko mice. 1, 3, and 6-month mice. N=6. ANOVA. No significant difference found.

DISCUSSION AND CONCLUSIONS

Male PMD patients with null mutations often do not exhibit motor and sensory symptoms until their 20's and they survive into their 50's (Raskind et al., 1991; Garbern et al., 1997; Inoue et al., 2002). Similarly, PLP deficient mice lack behavioral signs in their first year and have a nearly normal life span (Boison and Stoffel 1994; Klugmann et al., 1997). The myelin in these animals is essentially normal (Klugmann et al., 1997.) Thus, animals with a null mutation of the *PLP1/Plp1* gene have better outcomes compared to animals with extra copies or missense mutations of the wt*PLP1/Plp1* gene. These findings, along with the data showing that cellular abnormalities in *PLP1/Plp1* mutations are not limited to oligodendrocytes but include astrocytes, microglia (Tatar et al., 2010) and neurons, indicate that PLP plays an important role outside the myelin.

While the principal function of PLP is often considered to be that of an adhesive molecule in myelin (Boison et al., 1995), numerous studies show that PLP and DM20 have other functions (Nadon and West, 1998; Campagnoni and Skoff, 2001) including regulation of cell death (Skoff et al., 2004) and protein channel (Skoff, unpublished data). Recently, major oxidative phosphorylation defects in the *Plp1*tg mice have been described, specifically, a decrease in mitochondrial membrane potential and increase in extracellular ATP. This likely stems from an increase in PLP protein channels in mitochondria, though this has yet to be proven. Previous studies (Hüttemann et al., 2009; Appikalta et al., 2014) have found that when the *Plp1* gene is duplicated, PLP is inserted into the mitochondria utilizing unpaired twin C_X3C or C_X9C motifs that are present in the N-terminus of PLP. The metabolic defects due to the insertion of PLP into mitochondria are quite different from the commonly accepted view that PLP is exclusively a myelin

adhesive protein and that the pathology in the PLP mutants is due to demyelination and/or hypomyelination and are likely due to PLP playing a role as a protein channel in oligodendrocyte mitochondria (Skoff, unpublished data).

Major oxidative phosphorylation defects in neurons as well as oligodendrocytes (Hüttemann et al., 2009) in *Plp1*tg mice seem to lead to dramatic morphological changes of microglia, as well as an increase in expression of pro-inflammatory cytokines and chemokines (Tatar et al., 2010). Activation of microglia by increases in extracellular or exogenous ATP has been described in numerous studies (Gyoneva et al., 2009; Monif et al., 2009; Puthussery and Fletcher, 2009). Only a slight increase of ATP is needed to activate microglia. Exogenous ATP, in turn, activates microglial purinergic receptors (Davalos et al., 2005).

Here I have described, for the first time, an inflammatory response in *Plp1*ko mice. They, like *Plp1*tg mice, show intense microglial reactivity, thought to stem from mitochondrial dysfunction, though current data indicate otherwise. Although it remains to be determined whether and how the inflammation contributes to the neural degeneration in the PMD model mice, the well-known role of cytokine and chemokine activation in other neurodegenerative diseases makes it likely that microglial activation contributes to disease progression in *Plp1*tg mice and human patients.

We find that deletion of the *Plp1* gene leads to dramatic morphological changes of microglia. Changes include the shortening and thickening of microglial processes as well as an increased number, though not to the same extent as *Plp1*tg mice. The morphological changes in *Plp1*ko mice are as dramatic in the grey matter as in the white matter. This is like what was found in *Plp1*tg mice (Tatar et al., 2009). We found a

doubling of microglia throughout the cerebra of the *Plp1*ko mice and, as noted, these numbers are likely to be underestimated because microglia are densely clustered together. Data suggest that microglial activation is caused by other factors/molecules besides degeneration of myelin and is likely due to change in expression of PLP.

The intense microglial reactivity in *Plp1*ko mice suggested activation of multiple cytokines and chemokines. This is, however, not congruent with the low levels of oligodendrocyte cell death in *Plp1*ko mice (Skoff, et al, 2004). In *Plp1*tg mice mRNA expression of classical inflammatory markers TNF-α and IL-6 were elevated 24- and 7-fold respectively in 2-month-old animals. mRNA of nine other chemokines were elevated by more than 3-fold and several were down-regulated. For some of these chemokines such as CCL3/MIP-1a (macrophage inflammatory protein), its receptor (CCR1) is also up-regulated (Tatar et al., 2009). It is interesting that this is not the case in *Plp1*ko mice. Recall that pro-inflammatory cytokine/chemokine levels are either decreased or unchanged in these mice. Studies examining the microglia determine that *Plp1*tg mice have an M1 (cytotoxic) and *Plp1*ko mice have an M2 (neuroprotective) phenotype help to explain this.

Further studies are necessary to elucidate the mechanisms that lead to inflammation in the *Plp1*tg vs the *Plp1*ko mice, as well as downstream effects on neural function and morbidity to truly understand why a *Plp1*ko genotype is beneficial over a *Plp1*tg genotype for PMD patients.

REFERENCES

Appikatla S, Bessert D, Lee I, Hüttemann M, Mullins C, Somayajulu-Nitu M, Yao F, and Skoff RP. 2014. *Insertion of proteolipid protein into oligodendrocyte mitochondria regulates extracellular pH and adenosine triphosphate.* Glia. 62(3):356-73.

Bachstetter A, Webster S, Van Eldik L, and Cambi F. 2013. *Clinically relevent intronic splicing enhancer mutation in myelin proteolipid protein leads to progressive microglia and astrocyte actvation in white and grey matter regions of the brain.* J Neuroinflamm. 10:911.

Boison D and Stoffel W. 1994. *Disruption of the compacted myelin sheath of axons of the central nervous system in proteolipid protein-deficient mice.* Proc Natl Acad Sci. 22;91(24):11709-13.

Boison D, Bussow H, Urso D, Müller H, and Stoffel W. 1995. *Adhesive properties of proteolipid protein are responsible for the compaction of CNS myelin sheaths.* J Neurosci. 15(8):5502-13.

Boullerne A. 2017 *The History of Myelin.* Exp. Neurol. DOI: 10.1016/j.expneurol.2016.06.005

Butt A, Ibrahim M, Ruge F, and Berry M. 1995. *Biochemical subtypes of oligodendrocyte in the anterior medullary velum of the rat as revealed by the monoclonal antibody Rip.* Glia. 14(3):185-97.

Campagnoni A and Skoff RP. 2001. *The pathobiology of myelin mutants reveal novel biological functions of the MBP and PLP genes.* Brain Pathol. 11(1):74-91.

Cerget M, Bessert D, Nave K, and Skoff RP. 2009. *Sexual dimorphism in the white matter of rodents.* J Neurol Sci. 15;286(1-2):76-80.

Chen Z and TrappB. 2016. *Microglia and neuroprotection.* J Neurochem. 136 Suppl 1:10-7.

Cherry J, Olschowka J, and O'Banion M. 2015. *Arginase 1+ microglia reduce Aβ plaque deposition during IL-1β-dependent neuroinflammation.* J Neuroinflammation. 4;12:203.

Cherry J, Olschowka J, and O'Banion M. 2014. *Nueroinflammation and M2 microglia: the good, the bad, and the inflamed.* J Nueroinflammaton. 3;11:89.

Davalos D, Grutzendler J, Yang G, Kim J, Zuo Y, Jung S, Littman D, Dustin M, and Gan W. 2005. *ATP mediates rapid microglia response to local brain injury in vivo*. Nature Neuroscience 8(6);752-758.

Du L, Zhang Y, Chen Y, Zhu J, Yang Y, and Zhang H. 2017. *Role of Microglia in Neurological Disorders and Their Potentials as a Therapeutic Target.* Mol Neurobiol. 54(10):7567-84.

Garbern J. 2007. *Pelizaeus-Merzbacher disease: Genetic and cellular pathogenesis.* Cell Mol Life Sci. 64(1);50-65.

Gow A and Lazzarini R. 1996. *A cellular mechanism governing the severity of Pelizaeus-Merzbacher disease.* Nat Genet. 13:422-428.

Graeber M, Lopez-Redondo F, Ikoma E, Ishikawa M, Imai Y, Nakajima K, Kreutzberg G, and Kohsaka S. 1998. *The microglia/macrophage response in the neonatal rat facial nucleus following axotomy.* Brain Res. 7;813(2):241-53.

Gyoneva S, Orr A, and Traynelis S. 2009. *Differential regulation of microglia motality by ATP/ADP and adenosine.* Parkinsonism Relat Disord. 15 Suppl 3: S195-9.

Hüttemann M, Zhang Z, Mullins C, Bessert D, Lee I, Nave KA, Appikalta S, and Skoff RP. 2009. *Different proteolipid protein mutants exhibited unique metabolic defects.* ASN Neuro. 1(3):art:e00014. DOI:10.1042/AN20090028.

Imai Y, Ibata I, Ito D, Ohsawa K, and Kohsaka S. 1996. *A novel gene iba1 in the major histocompatibility complex class III region encoding an EF hand protein expressed in a monocytic lineage.* Biochem Biophys Res Commun. 25;224(3):855-62.

Inoue K, Osaka H, Thurston V, Clarke J, Yoneyama A, Rosenbarker L, Bird T, Hodes M, Shaffer L, and Lupski J. 2002. *Genomic rearrangements resulting in PLP1 deletion occur by nonhomologous end joining and cause different dysmyelinating phenotypes in males and females.* Am J Hum Genet. 71(4);838-53.

Ip C, Kroner A, Groh J, Huber M, Klein D, Spahn I, Diem R, Williams S, Nave K, Edgar J, and Martini R.. 2006. *Neuroinflammation by cytotoxic T-lymphocytes impairs*

retrograde axonal transport in an oligodendrocyte mutant mouse. J Neurosci. 26;8206-8216.

Ito D, Imai Y, Ohsawa K, Nakajima K, Fukuuchi Y, and Kohsaka S. 1998. *Microglia-specific localisation of a novel calcuim binding protein, Iba1.* Brain Res Mol Brain Res. 1;57(1):1-9.

Karperien A, Ahammer H, and Jelinek H. 2013. *Quantitating the subtleties of microglia morphology with fractal analysis.* Cell Neurosci. 30;7:3.

Klugmann M, Schwab M, Pühlhofer A, Schneider A, Zimmerman F, Griffiths I, and Nave K. 1997. *Assembly of CNS Myelin in the Absence of Proteolipid Protein.* Neuron. 18(1):59-70.

Koeppen A and Robitaille Y. 2002. *Pelizaeus-Merzbacher Disease.* J Neuropathol Exp Neurol. 61:747-759.

Laukka J, Kamholz J, Bessert D, and Skoff RP. 2016. *Novel pathological findings in patients with Pelizaeus-Merzbacher disease.* Neurosci Lett. 3;627:222-32.

Monif M, Reid C, Powell K, Smart M, and Williams D. 2009. *The P2X7 receptor drives microglia activation and proliferation: a trophic role for P2X7R pore.* J Neurosci. 25;29(12):3781-91.

Nadon N and West M. 1998. *Myelin proteolipid protein: function in myelin structure is distinct from its role in oligodendrocyte development.* Dev Neurosci. 20(6);533-9.

Nave K and Boespflug-Tanguy O. 1996.*X-Linked Developmental Defects of Myelination: From Mouse Mutants to Human Genetic Diseases.* The Neuroscientist. DOI: 10.1177/107385849600200111

Puthussery T and Fletcher E. 2009. *Extracellular ATP induces retinal photoreceptor apoptosis through activation of purinoreceptors in rodents.* J Comp Neurol. 1;513(4);430-440.

Raskind W, Williams C, Hudson L, and Bird T. 1991. *Complete deletion of the proteolipid protein gene (PLP) in a family with X-linked Pelizaeus-Merzbacher disease.* Am J Hum Genet. 49(6);1355-60.

Rath M, Muller I, KropfP, Closs E, and Munder M. 2014. *Metabolism via Arginase or Nitric Oxide Synthase: Two Competing Arginine Pathways in Macrophages.* Front Immunol. 27;5:532.

Readhead C, Schneider A, Griffiths I, and Nave K. 1994. *Premature arrest of myelin formation in transgenic mice with increased proteolipid protein gene dosage.* Neuron. 12:583-595.

Seitelberger F. 1995. *Neuropathology and genetics of Pelizaeus-Merzbacher disease.* Brain Pathol. 5:267-273.

Simons M, Kramer E, Macchi P, Rathke-Hartlieb S, Trotter J, Nave K, and Shulz J. 2002. *Overexpression of the myelin proteolipid protein leads to accumulation of*

cholesterol and proteolipid protein in endosomes/lysosomes: implications for Pelizaeus-Merzbacher disease. J Cell Bio. 157(2);327-336.

Skoff RP, Bessert, D, Cerghet M, Franklin M, Rout U, Nave K, Carlock L, Ghandour M, and Armant D. 2004.*The myelin proteolipid protein gene modulates apoptosis in neural and non-neural tissues.* Cell Death Differ. 11(12):1247-57.

Snaidero N and Simons M. 2017. *The Logistics of Myelin Biogenesis in the Central Nervous System.* Glia. 65(7):1021-31.

Tatar C, Appikalta S, Bessert D, Paintlia A, Singh I, and Skoff RP et al 2010. *Increased Plp1 gene expression leads to massive microglia cell activation and inflammation througout the brain.* ASN Neuro. 2(4): e00043.

Tonchev A, Yamashima T, Zhao L, and Okano H. 2003. *Differential proliferative response in the postischemic hippocampus temporal cortex, and olfactory bulb of young adult macaque monkeys.* Glia. 42(3):209-24.

Walker D and Lue L. 2015. *Immune phenotypes of microglia in human neurodegerative disease: challenges to detecting microglial polarization in human brains.* Alzheimers Res Ther. 7(1):56.

ABSTRACT

PROTEOLIPID PROTEIN 1 REGULATES INFLAMMATION IN THE CENTRAL NERVOUS SYSTEM

by

WHITNEY HOFF

May 2018

Advisor: Dr. Robert Skoff

Major: Molecular Genetics and Genomics

Degree: Master of Science

Pelizaeus-Merzbacher disease (PMD) results from mutations in the proteolipid protein 1 (*PLP1*) gene including *PLP1* duplications and deletions. The absence of PLP is preferable to *PLP1/Plp1* duplication in PMD patients and rodents as lifespan of *PLP1/Plp1* null mammals is nearly normal. The reason for this is not entirely understood. However, because of this, less attention has been placed on *Plp1* null mutations than on classical PMD mutations. However, data show that PLP levels must be properly titrated to ensure normal brain function. Specifically, changes in *PLP1/Plp1* expression can result in massive microglia activation in animal models of PMD and likely in human PMD patients. We asked if PLP plays a role in this activation and how. We hypothesized that PLP plays a necessary part in regulation of mitochondrial function and that a disturbance in PLP expression leads to an inflammatory response because of this. The purpose of this study was to investigate this hypothesis the *Plp1*ko mouse model as it has been studied previously in animals with excess PLP (*Plp1*tg mice). We found an extensive inflammatory response in *Plp1*ko as demonstrated by 2-3-fold increase in both the overall microglial

cell number in both male and female mice at 1, 3, and 6 months in *Plp1*ko mice. This increase can be accounted for by a 3-fold increase in microglial proliferation throughout the white and grey matter of the cerebra. Activity of microglia was quantified based on branching patterns of cell processes and the expression of CD68 (a marker for activated microglia). An increase in activation in *Plp1*ko mice is observable as early as 1 month and continues to at least 6 months. Interestingly, morphology of microglia and the effects of inflammation in *Plp1*ko mice differs from *Plp1*tg mice. A decrease in pro-inflammatory cytokines, as well as an increase in arginase 1 expression in *Plp1*ko mice, leads us to believe that while *Plp1*ko mice do experience an inflammatory response, microglia reactivity could be neuroprotective due to an alternative, or M2, activation state. This anti-inflammatory response would help to explain the benefits of *Plp1* deletion vs *Plp1* duplication. This study of *Plp1*ko mice, along with previous studies of *Plp1*tg mice, uncovers a novel function of PLP: regulation of brain inflammation, most likely mediated by the increase or absence of PLP in the mitochondria of oligodendrocytes. This must be understood in greater detail if we are to understand therapies for PMD and other diseased states.

AUTOBIOGRAPHICAL STATEMENT

Whitney Hoff

Education History

Masters of Science in Molecular Biology and Genomics May 2018
Wayne State University, Detroit, Michigan
Thesis: *Proteolipid Protein 1 Regulates Neuroinflammation in the Central Nervous System*
Advisor: Robert Skoff, PhD
GPA: 3.54

Bachelor of Science in Biology, minor in Chemistry
Southern Utah University, Cedar City, Utah
Summa Cum Laude, GPA: 3.87

Employment History

Graduate Research Assistant Aug 2012-Present
Wayne State University, Detroit, Michigan
Supervisor: Robert Skoff, PhD
Tasks: immunocytochemistry, microscopy, quantitative analysis, western blotting, solution preparation, grant writing, manuscript preparation, general research

Chemistry Teaching/Laboratory Assistant Aug 2009-Aug 2012
Southern Utah University, Cedar City, Utah
Supervisors: Kristina Bronsema; Kim Weaver, PhD; Daniel Eves, PhD; McKay Steffensen, PhD
Tasks: supervising up to 40 students, tutoring students in general and organic chemistry, grading laboratory write ups, assisting with laboratory experiments, setting up laboratory experiments, proctoring exams, teaching of weekly organic chemistry review sessions

Publications

Proteolipid Protein 1 Regulates Neuroinflammation in the Central Nervous System 2018
Hoff W, Bessert D, Yao F, Skoff R

Duplication of PLP, Not DM20, Causes Apoptosis in Oligodendrocytes by Inducing Mitochondrial Dysfunction in Pelizaeus Merzbacher Disease 2018
Somayajulu M, Bessert D, Hoff W, Hüttemann M, Yao F, Skoff R

Professional Associations

American Society for Neurochemistry
Member since 2015

Society for Neuroscience Michigan Chapter
Member since 2017